

Isospin violation in the πN system at low energies

E. Matsinos*

Institute for Particle Physics, ETH Zurich, CH-5232 Villigen PSI, Switzerland

(Received 6 June 1997)

The low-energy πN interaction is investigated with the use of a relativistic isospin-symmetric πN model based on scalar-isoscalar and vector-isovector exchanges in the t channel, and the nucleon and Δ -isobar contributions in the s and u channels; the small contributions from the well-established s and p higher (baryon) resonances are also taken into account. In the region of elasticity, the model provides a firm basis for analyzing the experimental data. The analysis of all (recent and old) πN measurements between (pion laboratory kinetic energy of) 20 and 100 MeV has been achieved with the implementation of robust statistics. Provided the correctness of the bulk of the experimental data and the completeness of the electromagnetic corrections applied to the scattering problem, this work provides overwhelming evidence for isospin-symmetry breaking of the strong interaction in the πN system. [S0556-2813(97)03212-3]

PACS number(s): 13.75.Gx, 11.30.Hv, 25.80.Dj

I. INTRODUCTION

The construction of the three meson factories (LAMPF, PSI, and TRIUMF) inaugurated a new era in the experimental and theoretical investigation of the pion-nucleon (πN) system. The existence of an abundance of measurements now permits one to delve into the question of the low-energy structure of the theory of the strong interactions, i.e., of the quantum chromodynamics (QCD); one of the principle features of QCD is that chiral and isospin symmetry are almost exact properties of its Lagrangian.

The quark masses are free parameters in QCD; at low energies, only the light (u and d) quarks are important. The amount of breaking of isospin symmetry in the strong interaction is expected to lead to a precise determination of the light-quark masses [1].

The usefulness of an analysis of the low-energy (pion laboratory kinetic energy $T_\pi \leq 100$ MeV) πN data in this context is twofold. (a) At low energies, QCD is highly non-perturbative. Due to this reason, an effective-field approach (respecting the properties of the QCD Lagrangian) has been put forward (for a recent review, see Refs. [1]) to account for the (low-energy) hadronic phenomena; the chiral-perturbation theory (χ PT). The lower the energy is, the better χ PT is expected to work (the effective Lagrangian is expanded in a Taylor series in the momenta involved). The physical quantities, describing the interaction at low energies, start now to become accessible to calculations performed within the framework of χ PT, e.g., see Ref. [2]. (b) The lower the energy is, the more important the isospin-breaking effects are expected to become. This is due to the fact that the (kinetic) energies, associated with the interaction, become then comparable to the difference of the masses of the u and d quarks.

The advantages of an *exclusive* analysis of the low-energy πN data originate from the simplicity of the interaction there [3]; the contributions from the higher resonances (that is, other than the Δ_{33}) are small, the inelasticities are negligible,

the higher partial waves (i.e., other than s and p) are tiny, and, finally, there is no need for the introduction of form factors.

It was shown in Ref. [3] that a relativistic isospin-symmetric model consisting of scalar-isoscalar and vector-isovector t -channel exchanges, along with the nucleon and the Δ -isobar s - and u -channel graphs could account for the πN phase shifts (at least) up to the energy of the Δ_{33} resonance. The model also provided a method for the determination of the relevant low-energy hadronic constants; in that work, the parameter values were obtained from fits to the Karlsruhe-Helsinki (KH80) phase-shift solution [4], which is (almost exclusively) based on measurements conducted in the pre-meson-factory era.

In the present work, the principle aim is the investigation of the isospin symmetry of the strong interaction in the πN system at low energies. This goal will be achieved in the following two steps.

(a) The internal consistency of the data in the three low-energy experimentally accessible πN channels, i.e., the two elastic-scattering processes ($\pi^\pm p$) and the single-charge-exchange (SCX) reaction ($\pi^- p \rightarrow \pi^0 n$), will be investigated. Each of these reactions will be analyzed *separately*. Robust statistics will be implemented in the problem. With the exception of a few measurements which (almost entirely) pertain to the $\pi^+ p$ set, the internal consistency of the data base will be proven.

(b) The hadronic amplitudes obtained at step (a) (as well as the one obtained from a combined analysis of the measurements in the two elastic-scattering channels) will be compared. The principle of isospin symmetry imposes a specific restriction to these amplitudes (e.g., see the Appendix, part 1), the fulfillment of which will be examined.

II. THE πN MODEL

The extended tree-level model of Ref. [3] exploits an important feature of the πN dynamics, i.e., *the weakness of the interaction at low energies*. Herein, it has been generalized with the inclusion of the derivative coupling of the scalar-

*Electronic address: evangelos.matsinos@psi.ch; Tel.: +41 56 310 32 77, FAX: +41 56 310 43 62.

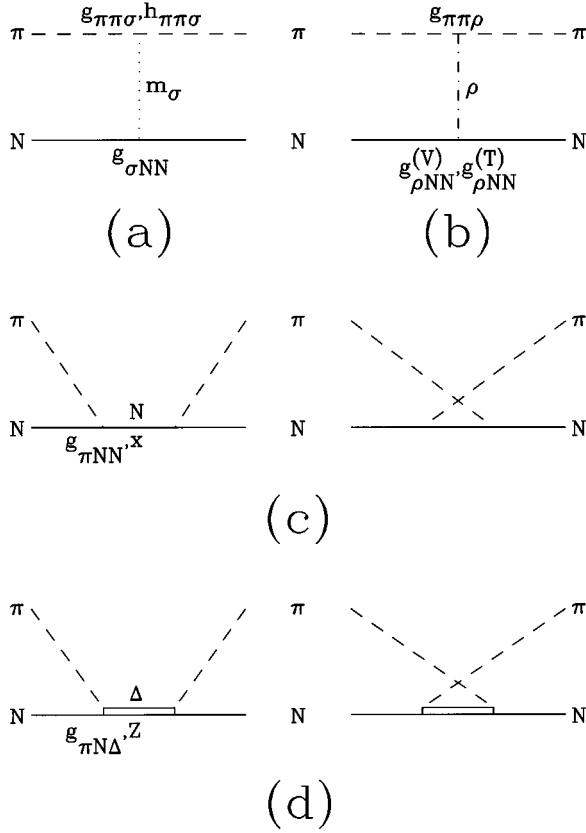


FIG. 1. (a) The t -channel scalar-isoscalar exchange, (b) the t -channel vector-isovector exchange, (c) the s - and u -channel graphs with a nucleon in the intermediate state, and (d) the s - and u -channel graphs with a Δ isobar in the intermediate state.

isoscalar to the pion field. The interaction Lagrangian, corresponding to the $\pi\pi\sigma$ vertex, takes the form

$$\Delta\mathcal{L}_{\sigma\pi\pi} = -g_{\pi\pi\sigma}m_{\pi}\boldsymbol{\pi}\cdot\boldsymbol{\pi}\phi + \frac{h_{\pi\pi\sigma}}{m_{\pi}}\partial_{\mu}\boldsymbol{\pi}\cdot\partial^{\mu}\boldsymbol{\pi}\phi. \quad (1)$$

The ratio of the two coupling constants is denoted by κ_{σ} ($=h_{\pi\pi\sigma}/g_{\pi\pi\sigma}$). Exempting the newly added coupling, all details about the model may be found in Ref. [3]. The (essential) contributions to the πN scattering amplitude are shown (in the form of Feynman diagrams) in Figs. 1. Four partial waves (s , p , d , and f) have been considered herein; in the energy region assumed in the present analysis, only the s - and p -wave contributions are important.

The model parameters (to be determined from the πN data) are the following:

(a) G_{σ} and κ_{σ} , relating to the scalar-isoscalar t -channel exchange,

(b) G_{ρ} (defined as $G_{\rho}^{(V)}$ in Ref. [3]) and κ_{ρ} (defined as κ in Ref. [3]), relating to the vector-isovector t -channel exchange,

(c) $g_{\pi NN}$ and x , respectively, denoting the πNN coupling constant and the pseudoscalar admixture in the πNN vertex, and

(d) $g_{\pi N\Delta}$ and Z , the former denoting the $\pi N\Delta$ coupling constant, the latter being associated with the spin-1/2 admixture in the Δ -isobar field.

All other physical constants have been fixed at the values recommended by the particle data group [5]. m_{π} was fixed at the charged-pion mass. For reasons of compatibility with the method incorporating the electromagnetic corrections (see Sec. IV A), the proton mass m is assigned to the nucleon. The range of the scalar-isoscalar interaction m_{σ} was obtained from $\pi\pi$ phase shifts;¹ $m_{\sigma}=860$ MeV/ c^2 [6]. The small contributions from the well-established (four-star) s and p higher (baryon) resonances (with masses up to 2 GeV/ c^2) have also been taken into account; the states considered are: $P_{11}(1440)$, $S_{11}(1535)$, $S_{11}(1650)$, $P_{13}(1720)$, $S_{31}(1620)$, and $P_{31}(1910)$. The higher resonances do not introduce any free parameters.

The πN model, thus constructed, contains the exchange of $I=J=0$ and $I=J=1$ mesons in the t channel, and all the well-established intermediate states below 2 GeV/ c^2 in the s and u channels. Possible contributions from higher resonances, other than the ones considered herein, are bound to be negligible.

III. THE EXPERIMENTAL DATA

The low-energy πN data base consists of measurements in three reaction channels, i.e., in the two elastic-scattering processes and in the SCX channel. Measured are the following physical quantities:

(a) Differential cross sections $d\sigma/d\Omega$.

(b) Partial-total cross sections σ_{pt} : Determined is the percentage of the projectiles (pions), scattered between a minimal laboratory scattering angle θ_L^{\min} and 180° . Since the determination of the beam attenuation involves the detection of a charged pion in the final state, the total SCX cross section is almost entirely included in the $\pi^-p\sigma_{pt}$ measurements.

(c) Total nuclear cross sections σ_t : The raw partial-total cross sections (for several values of θ_L^{\min}) are first corrected for major electromagnetic effects (the contributions of the Coulomb peak and the Coulomb-nuclear interference); σ_t is defined as the extrapolated value to $\theta_L^{\min}=0^\circ$.

(d) Polarization or analyzing power A : Differential cross sections on polarized targets are measured; the observable is defined as the asymmetry ratio (difference in the spin-up and spin-down results divided by their sum).

In the present analysis, included in the data base are *all*² published πN experimental data (737 data points) between 20 and 100 MeV. The low-energy limit, assumed herein, is dictated by the applicability region of the algorithm incorporating the electromagnetic corrections. The π^-p partial-total and total nuclear cross sections (nine entries in the energy interval under consideration) have to be excluded, because they contain the (larger) total SCX cross section (thus, mingling properties of two reaction channels). Let us now come to a short description of the individual data sets comprising the data base.

¹The whole analysis was repeated with m_{σ} fixed at 600 MeV/ c^2 . The changes, thus induced in the results, were found to be insignificant.

²Only the six measurements of $d\sigma/d\Omega$ of Ref. [7], which have been taken close to 100 MeV, were excluded; they have not appeared in a form permitting their (straightforward) inclusion.

A. The data in the elastic-scattering channels

$d\sigma/d\Omega$: The data base consists of the recent measurements (Refs. [8–15]), the data of Bertin *et al.* [16], Auld *et al.* [17], and Ritchie *et al.* [18]. In order to treat all data sets at the same footing, the individual contributions to the normalization uncertainty in the measurements of Ref. [11] were summed quadratically [19].

σ_{pt} : Data on the σ_{pt} were published in Ref. [20]. Subsequently, the two lowest-energy entries were withdrawn [21] and the results of a reanalysis, including the effects of a beam-energy calibration at TRIUMF, became available recently [22]; herein, the values of Ref. [22] are used. The very recent measurements from LAMPF [23] have also been included.

σ_t : Included are the data of Carter *et al.* [24] and Pedroni *et al.* [25].

Analyzing power: The data base comprises the recent measurements of Ref. [26] (at 68.34 MeV), and the measurements of Refs. [27] and [28] (at 98 MeV).

B. The data in the SCX channel

Measurements of $d\sigma/d\Omega$ have been published in Ref. [29]; they have been taken in the region of the (s - and p -wave) destructive-interference dip. Past measurements of $d\sigma/d\Omega$ at 180° were published in Ref. [30]. The first three coefficients in the expansion of $d\sigma/d\Omega$ in a Legendre series have been obtained at six energies in Refs. [31] and [32]. The earlier measurement [33] of σ_t at 90.9 MeV and the four measurements of the analyzing power at 100 MeV from TRIUMF [34] have also been included in the data base.

Unfortunately, no results from the reanalysis of older experimental data (of $d\sigma/d\Omega$), taken at LAMPF (experiment code number: 882), are yet available [35]. Some additional measurements of $d\sigma/d\Omega$ (also from LAMPF) at 27.5 MeV are in a nearly-final state [36]. These values are expected to appear soon.

IV. THE ANALYSIS

A. The method

Followed is the K -matrix formalism [3]. The K -matrix elements, obtained from the diagrams of Figs. 1 (also adding the small contributions from the s - and u -channel graphs with the higher resonances in the intermediate state), are related to the corresponding hadronic phase shifts $\delta_\alpha(\epsilon)$ via the equation

$$k \cot(\delta_\alpha(\epsilon)) = K_\alpha^{-1}(\epsilon), \quad (2)$$

where the index α stands for the total isospin, orbital, and total angular momentum of the particular channel; k and ϵ denote the pion center-of-mass (c.m.) momentum and kinetic energy, respectively.

From the hadronic phase shifts to the level of the πN observables, the NORDITA algorithm has been strictly followed [37]. The corrections to the phase shifts and the (small) inelasticities have been obtained from the tabulated values of Refs. [37] via simple interpolations. The hadronic phase shifts $\delta_\alpha(\epsilon)$, obtained from the K -matrix elements of the model via Eq. (2), lead to the (so-called) nuclear phase

shifts $\delta_\alpha^N(\epsilon)$. The nuclear phase shifts are used to construct the (partial-wave) nuclear amplitudes (the Coulomb phase shifts are also taken into account). Finally, the spin-non-flip (G) and the spin-flip (H) amplitudes are obtained (after the pure Coulomb contributions are added); all the interesting physical quantities (differential cross sections, partial-total and total nuclear cross sections, analyzing powers, and spin-rotation parameters) may be easily determined in terms of these amplitudes (e.g., see Refs. [37] and [3]).

The πN scattering amplitude, constructed on the basis of the model, obeys the first principles of unitarity, analyticity,³ Lorentz invariance, and crossing symmetry. In the context of the aim of the present work, the advantages of the method, implemented herein, over the (traditionally used) dispersion-relation schemes are important.

(a) The values of the model parameters are obtained from low-energy data exclusively.

(b) Separate analyses of the experimental data in any of the three reaction channels are possible.

(c) The attribution of uncertainties to the important quantities in this analysis is straightforward.

B. The modeling of the data

Inconsistencies among the low-energy πN experimental data have been discussed extensively over the past years [38]; they may be classified into two categories.

(a) True discrepancies, involving measurements in *one* reaction channel and taken at similar kinematical conditions. Of course, the relevant question here is: Which of the two (or more) experiments is (are) correct? *Robust statistics* [39] can provide the answer to this question; the outliers (discrepant measurements) are easily detected on the basis of their deviation from the *bulk* of the data.

(b) Spurious discrepancies, involving experimental data in *different* reaction channels. Such effects may be physical if the assumptions, underlying the data analysis (e.g., isospin symmetry), are not valid.

In the present work, a (maximum likelihood) local M estimator, which emerges (in a natural way) from the features of the experimental data, will be used. Let us introduce the variable z (normalized residual), defined for the i th entry of a series of N measurements as

³It was recently stated by G. Höhler that a tree-level model cannot fully reproduce the properties of πN amplitude in the unphysical region. The remark relates to the cusp effect at $t=4m_\pi^2$ (t is the standard Mandelstam variable); indeed, the πN amplitude, constructed on the basis of the present model, is a smooth function of two kinematical variables. However, fitting the model to the KH80 phase-shift solution [4], one obtains a value for the $\pi N \Sigma$ term (tree-level approximation) which is very close to what R. Koch extracted in 1982 based on the *same* phase shifts and using dispersion relations (in which the cusp effect is contained); 62.5 ± 5.5 MeV as compared to his 64 ± 8 MeV, e.g., see Ref. [3]. This fact might serve as an indication that the cusp effect in the unphysical region does not substantially modify the extrapolation to the Cheng-Dashen point; its influence in the physical region (which lies further away from $t=4m_\pi^2$) is expected to be negligible.

$$z_i = \frac{y_i - y_i^{\text{exp}}}{\delta y_i^{\text{exp}}}, \quad (3)$$

where y_i is the optimal value estimated on the basis of the parametric model, y_i^{exp} denotes the measured value, and δy_i^{exp} is the uncertainty of the measurement. In a statistical analysis, the distribution of $z(\psi(z))$ for the measurements involved is of great importance. Under the assumption that the measurements are independent, the joint probability density function takes the form

$$\mathcal{F}(\mathbf{p}) = \prod_{i=1}^N \psi(z_i), \quad (4)$$

\mathbf{p} denoting the parameter vector to be optimized. Sought is the maximization of $\mathcal{F}(\mathbf{p})$ or (equivalently) of its natural logarithm

$$\ln \mathcal{F}(\mathbf{p}) = \sum_{i=1}^N \ln \psi(z_i). \quad (5)$$

It is easy to verify that if z is normally distributed (as expected from the laws of statistics, i.e., from the central-limit theorem), then maximizing $\ln \mathcal{F}(\mathbf{p})$ is equivalent to minimizing the standard χ^2 function ($= \sum_{i=1}^N z_i^2$). However, in the case of the low-energy πN measurements, z was found to follow a *Cauchy distribution* (see Fig. 2),

$$\psi(z) \sim \frac{1}{1+z^2}, \quad (6)$$

dictating the minimization of the function

$$\text{MF} = \sum_{i=1}^N \ln(1+z_i^2). \quad (7)$$

At this point, one has to remark that there is no theoretically justified reason that the distribution of z should be a Lorentzian instead of a Gaussian; the deviation from the Gaussian distribution signifies either an insufficient parametric model or experimental flaws. It is also important to note that the distribution of z and the choice of the minimization function are, in principle, linked [i.e., if $\psi(z)$ is a Lorentzian, then one should not minimize a χ^2 function⁴]. In reality, however, the more robust a method is, the less crucial the choice of the exact form of the estimator becomes [39], e.g., there is no danger in applying a robust technique in the modeling of data with normally distributed z . In the present analysis, the standard MINUIT routines [40] of the CERN library have been used throughout the optimization phase.

One word about the uncertainties in the experimental values is prompt. *The uncertainty δy_i^{exp} , appearing in Eq. (3), should, in principle, be the random uncertainty of the i th entry.* However, the uncertainties, relating to the majority of the old experiments, correspond to the quadratic combination of random and systematic effects; the information about the

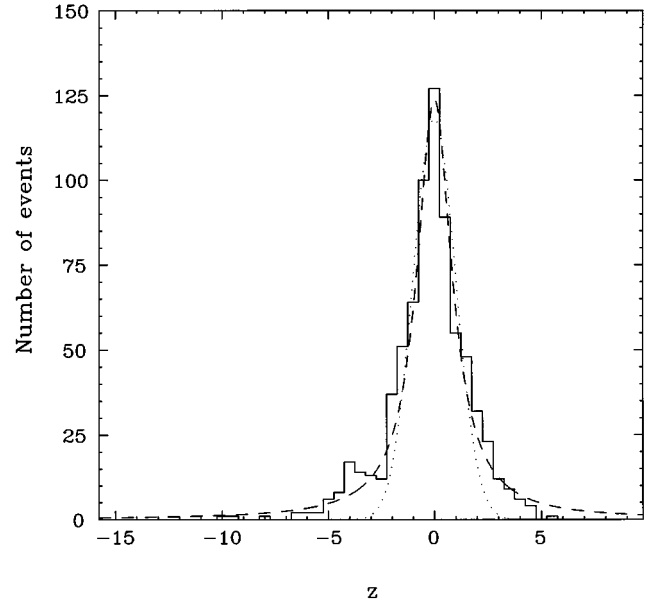


FIG. 2. The distribution of z [see Eq. (3)] for the low-energy πN measurements (used as input). The best Cauchy (dashed curve) and the best normal (dotted curve) fits are also shown.

breakdown of the two components is lost, thus, disabling the elaborate statistical analysis of Ref. [41] (which was recently carried out for the case of the meson-factory $\pi^+ p$ differential-cross-section measurements). In order to avoid the introduction of bias in the present work, random and systematic uncertainties were combined (quadratically) for all entries. It is true, of course, that the entries in one particular data set are all subject to the same treatment under normalization (i.e., all have to be scaled upwards or downwards by the same amount in order to meet the optimal solution). However, a reasonable assumption might be that the effects of the normalization cancel out for a large number of data sets, especially so provided the diversity of the experimental techniques, groups, places, and times. In other words, the systematic uncertainties should behave like random uncertainties for a large number of independent experiments.

C. The determination of the πN amplitudes

Two isospin-breaking processes in the πN system have, up to now, been considered in the literature (Refs. [42–44]); they are based on the ρ^0 - ω and η - π^0 mixing mechanisms. Both are put to work in the vector-isovector t -channel graph, the latter one also affects the s and u channels. In both cases, *the scalar-isoscalar interaction is unaffected*, thus, enabling the extraction of the three relevant πN hadronic amplitudes $f_{\pi^+ p}(\epsilon)$, $f_{\pi^- p}(\epsilon)$, and $f_{\text{SCX}}(\epsilon)$ (for details, see the Appendix, part 1) with the implementation of the following strategy.

(a) Fits to the $\pi^- p$ scattering data are carried out varying G_ρ between 30 and 60 GeV^{-2} (a step of 5 GeV^{-2} having been assumed); this interval corresponds to the extreme values found in the literature (e.g., see Ref. [3]). The $\pi^- p$ scattering amplitude $f_{\pi^- p}(\epsilon)$ is constructed on the basis of 262 data points. The fits to the data involve the variation of seven model parameters (i.e., all, except for G_ρ).

⁴Exceptions mark the domain of applicability of the Gauss-Markov theorem.

(b) All attempts to obtain the π^+p scattering amplitude $f_{\pi^+p}(\epsilon)$ from the data, following the procedure of case (a), failed; the corresponding error matrices were not positive definite, thus, marking the results of the fits as unreliable. This failure is due to the fact that only one isospin amplitude is present in the π^+p channel; this results in high correlations among the model parameters. In order to enable a reliable extraction of $f_{\pi^+p}(\epsilon)$, one or more model parameters had to be fixed. On the basis of the fact that the scalar-isoscalar interaction is unaffected by the ρ^0 - ω and η - π^0 mixing mechanisms, the two parameters G_σ and κ_σ were fixed, for each particular G_ρ value, at the corresponding values obtained from the π^-p fits of case (a). Fits to the π^+p scattering data were thus attempted for the seven G_ρ values and the π^+p scattering amplitude $f_{\pi^+p}(\epsilon)$ was successfully constructed from 428 data points. In the π^+p case, the fits to the data involve the variation of five model parameters for each G_ρ value.

(c) Fits to the SCX scattering data were also performed for the seven G_ρ values. Since the scalar-isoscalar interaction cannot produce a neutral pion in the final state (starting from a charged projectile), the two parameters G_σ and κ_σ were fixed at zero. The SCX scattering amplitude $f_{\text{SCX}}(\epsilon)$ is constructed on the basis of 47 data points. The fits to the data involve the variation of five model parameters for each G_ρ value.

In all three cases (a)–(c), healthy minima were obtained.

Combined fits to the measurements in the two elastic-scattering channels were also performed for the seven values of G_ρ . In principle, one may blame any of the three reaction channels for possible deviations from the principle of isospin symmetry. However, the ρ^0 - ω and η - π^0 mixing mechanisms seem to be “biased” against the SCX channel; only one diagram (see Refs. [43] and [44]) for isospin breaking in the elastic-scattering channels has been put forward,⁵ whereas at least five graphs are potentially present in the case of the SCX channel. The simultaneous description of the data in the two elastic-scattering channels was achieved and the amplitude $f_{\pi^\pm p}(\epsilon)$ was constructed on the basis of 690 data points. The fits to the data involve again the variation of seven model parameters (i.e., all, except for G_ρ). In every case, a healthy minimum was obtained.

In all the above cases, equally good descriptions of the data are obtained for all G_ρ values.

In the following, the model predictions for the various observables, amplitudes, etc., are determined via Monte Carlo simulations, in which the results of the corresponding fits (i.e., parameter values, errors, and the correlation matrices) are fully taken into account.

V. RESULTS AND DISCUSSION

A. Reproduction of the data

Shown in Figs. 3 are the z distributions corresponding to the measurements in each of the three reaction channels; they

⁵Provided that the assumptions of Ref. [44] about the ρ^0 - ω dynamics are valid, the contributions from this mechanism to the amplitudes at threshold (zero kinetic energy of the incident pion) are actually only about *half* of what they are claimed to be in Ref. [44] due to a conversion error.

have been obtained from the results of the separate fits to the data [steps (a)–(c), see previous section]. The composition of the tails of these distributions, defined by the condition $|z| > 3$, was investigated.

(a) π^+p case: about 17% of the data occupy the tails of the z distribution. 61% of the BERTIN76 data [16] (i.e., 58% of all measurements satisfying $|z| > 3$), along with the two CARTER71 measurements [24], populate the lower tail of the distribution. The use of the data of Refs. [16] and [24] in *nonrobust* optimizations certainly leads to very precarious results. One-third (eight entries) of the BRACK86 data [9] belong to the upper tail of the z distribution. It should also be mentioned that two of the recent data sets (the BRACK90 66.8 MeV [12] and the JORAM95 32.7 MeV [14] measurements) have a shape which is in sheer contradiction with the bulk of the measurements.

(b) π^-p case: 5% of the data base (a total of 13 entries) correspond to the tails of the distribution. The WIEDNER89 data set [11] yields more than half of these points.

(c) SCX case: no entry satisfies the condition $|z| > 3$; the SCX data base is internally consistent.

In retrospect, the following conclusions may be drawn:

(a) The low-energy πN data base becomes internally consistent in case that one rejects the true outliers which are present almost exclusively in the π^+p channel.

(b) It may be easily deduced from Fig. 3(b) that, in the case of the elastic π^-p channel, the measurements can be (equally well) described by both a Cauchy and a normal form. With the exception of a few measurements, the π^-p data base is internally consistent.

(c) Although a statistical analysis of the SCX measurements is impossible due to the smallness of the sample, no outliers were seen in this channel [Fig. 3(c)].

A thorough investigation of the reproduction of the input data may be found elsewhere [45].

B. Isospin symmetry

Since the phase shifts vanish at the πN threshold, a more useful representation of the reaction dynamics (close to threshold) is achieved in terms of the low-energy form of the πN scattering amplitude (see the Appendix, part 2). The results for the real parts of the corresponding s - and p -wave isoscalar and isovector coefficients are shown in Fig. 4 for three typical energies. The comparison of these values is based on the philosophy put forward in Refs. [46]. Provided that isospin is a good symmetry in the πN system, then the entire information, concerning the three low-energy reaction channels, is contained in *six* (energy-dependent) complex functions [i.e., in the coefficients $b_0(\epsilon), \dots, d_1(\epsilon)$]. In such a case, (a) the π^+p process provides (and is described by) the combinations $b_0(\epsilon) + b_1(\epsilon)$, $c_0(\epsilon) + c_1(\epsilon)$, and $d_0(\epsilon) + d_1(\epsilon)$ (in Fig. 4, the reaction is represented by the vertical bands), (b) the π^-p process yields the combinations $b_0(\epsilon) - b_1(\epsilon)$, $c_0(\epsilon) - c_1(\epsilon)$, and $d_0(\epsilon) - d_1(\epsilon)$ (in Fig. 4, the reaction is represented by the horizontal bands), and (c) the SCX is directly related to $b_1(\epsilon)$, $c_1(\epsilon)$, and $d_1(\epsilon)$ (in Fig. 4, the reaction is represented by the diagonal bands). At any energy, the principle of isospin symmetry necessitates a common overlap of the three corresponding bands.

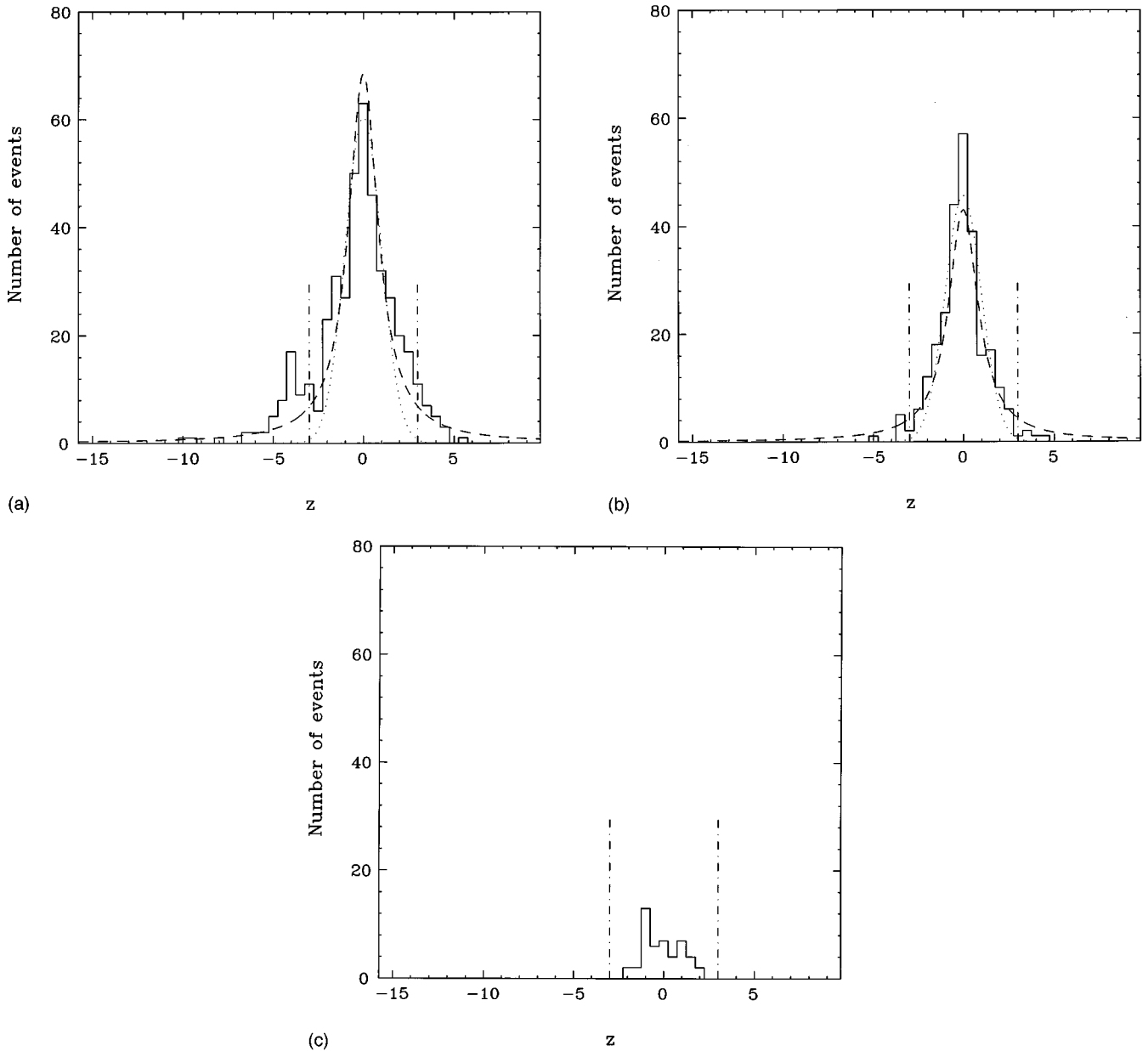


FIG. 3. The z distributions corresponding to the measurements in the three low-energy experimentally accessible πN channels; (a) $\pi^+ p$, (b) $\pi^- p$, and (c) SCX data. They have been obtained from the results of the separate fits to the measurements. The best Cauchy (dashed curves) and normal (dotted curves) descriptions of the data are also shown. The dash-dotted lines mark the limits corresponding to the condition $|z| > 3$ (see Sec. V A).

Figure 4 provides indications that the isospin symmetry of the strong interaction is broken in the πN system. As easily seen in this figure, the bands, resulting from the separate analyses of the data in the three reaction channels, are relatively wide; unfortunately, an isospin-breaking effect cannot be established beyond doubt on the basis of their comparison. It was found, however, that the combined fits to the elastic-scattering data lead to smaller uncertainties. This is understood on the basis of the following argumentation. In the case of the exclusive $\pi^- p$ analysis, both isospin amplitudes are present in the scattering and, thus, have to be determined from single-channel data; the determination is not very precise due to their correlation (see the Appendix, part 1). In a combined analysis of data in the two elastic-scattering channels, the isospin- $\frac{3}{2}$ amplitude is (almost en-

tirely) fixed from the $\pi^+ p$ reaction, leaving only the isospin- $\frac{1}{2}$ amplitude to be determined from the $\pi^- p$ data; thus, both isospin amplitudes are accurately determined.

The results of the combined fits to the elastic-scattering data are shown in Fig. 5 along with the results obtained from the SCX data. The lack of a common solution manifests a strong violation of isospin symmetry in the s -wave part of the interaction. The relative difference in the real parts of the two s -wave amplitudes amounts to $6.4 \pm 1.4\%$ (average over the three typical energies). This is a clear and overwhelming evidence that isospin symmetry of the strong interaction is broken in the πN system around 50 MeV.

The sensitivity of this result to the existence of outliers among the input data was carefully investigated. The whole analysis was repeated after the measurements of Refs. [16]

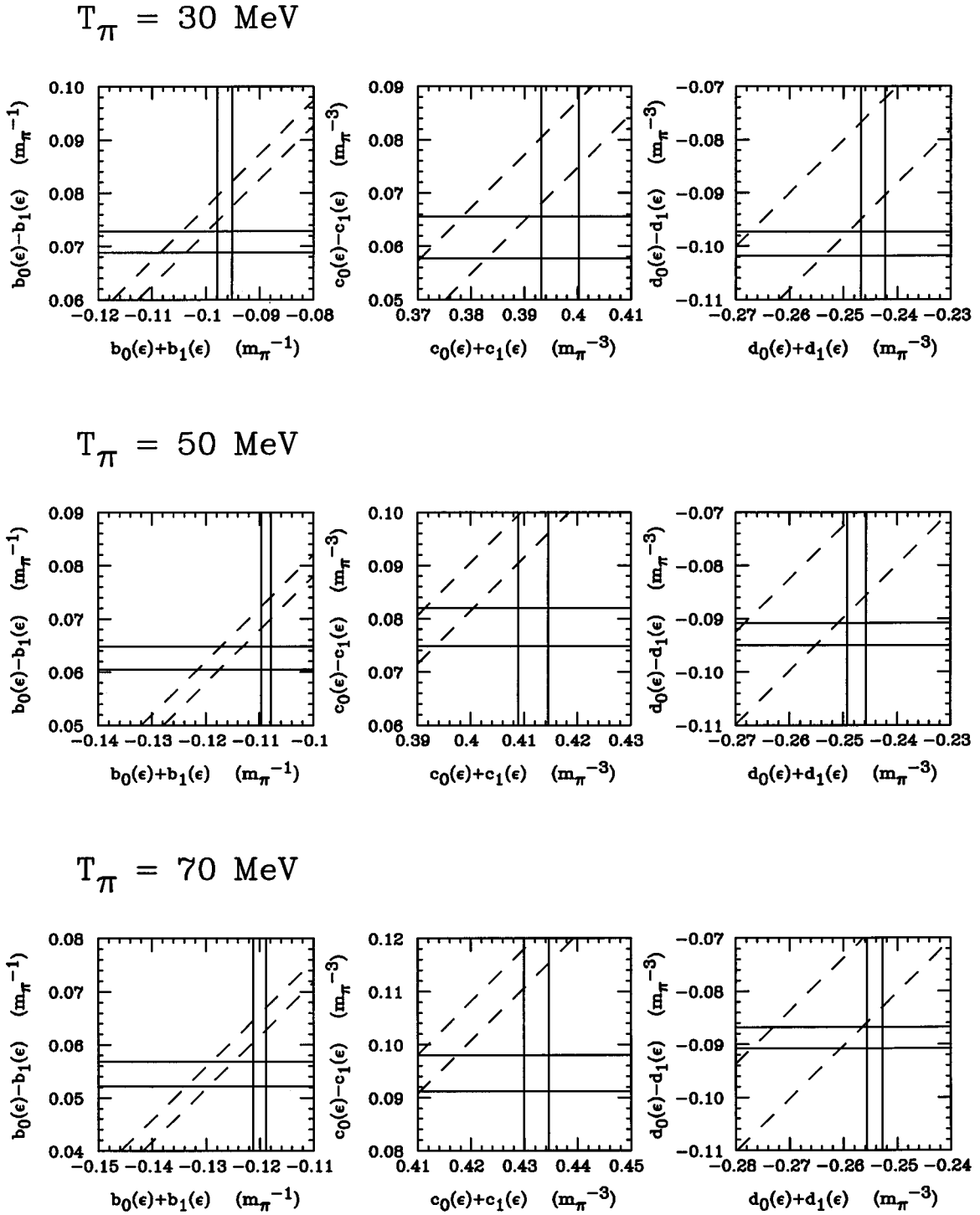


FIG. 4. The real parts of the s - and p -wave isoscalar and isovector coefficients of the low-energy form of the πN scattering amplitude (see the Appendix, part 2) for three typical energies. The π^+p process is represented by the vertical bands, the π^-p process by the horizontal bands, and the SCX reaction by the diagonal bands.

and [24] were removed from the data base. The changes, thus induced, were found to be insignificant.

In order to examine the sensitivity of the effect to the electromagnetic corrections, the whole analysis was repeated after the corrections to the hadronic phase shifts, the inelasticities, and the isospin-mixing amplitudes (see Ref. [37]) were omitted; thus, only the pure Coulomb amplitude and the Coulomb phase shifts were taken into account. The difference in the real parts of the two s -wave amplitudes, re-

sulting from the combined fits to the elastic-scattering measurements and from the ones to the SCX data, is now slightly larger (difference of one-and-a-half standard deviations) than the case where the NORDITA algorithm is strictly followed. Therefore, the main conclusion of the present work might only be affected in the case where the electromagnetic corrections of Ref. [37] are largely erroneous.

It should be noted that Gibbs, Ai, and Kaufmann [47] have also investigated the subject of the present analysis.

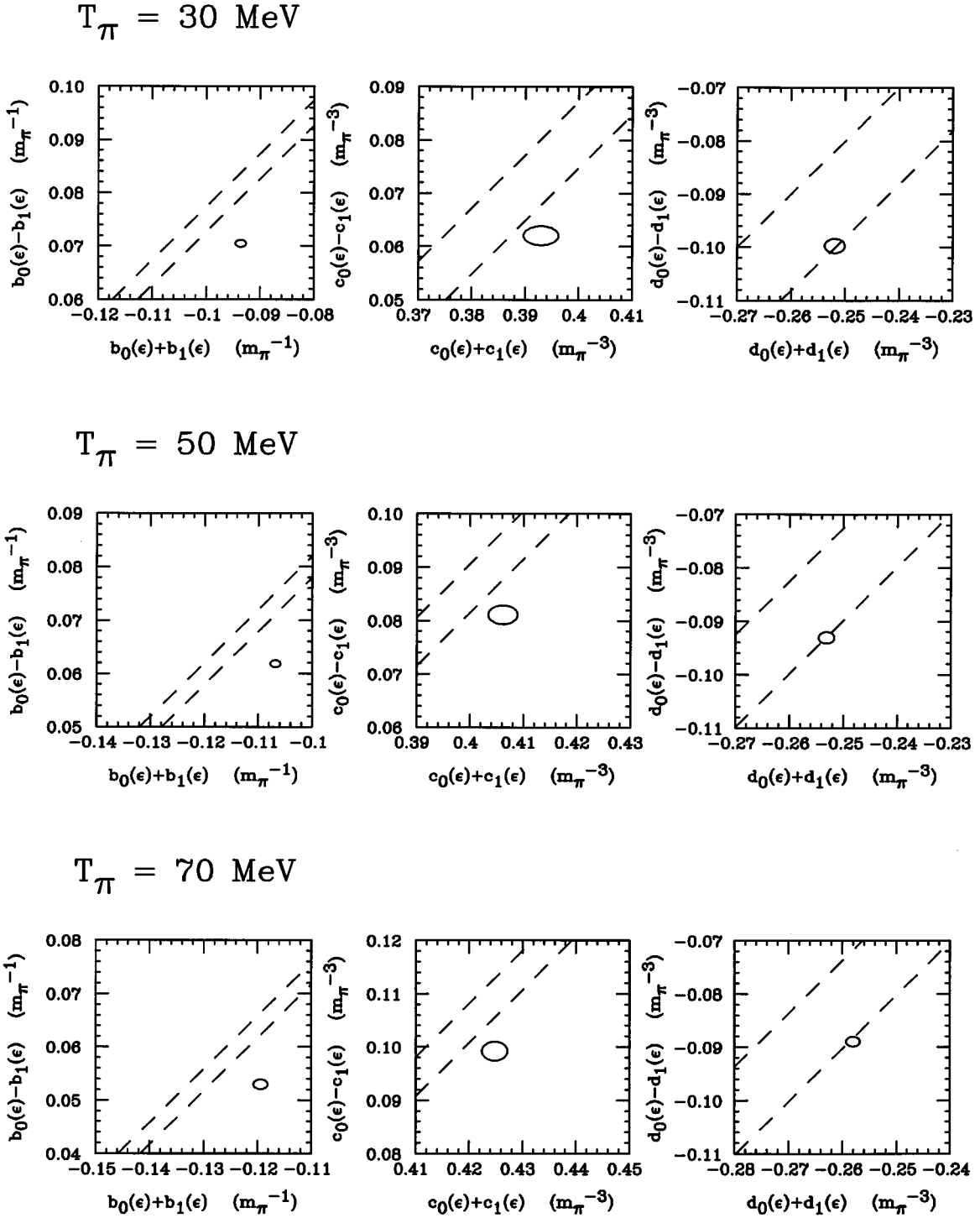


FIG. 5. The real parts of the s - and p -wave isoscalar and isovector coefficients of the low-energy form of the πN scattering amplitude (see the Appendix, part 2) for three typical energies. The SCX reaction is represented by the diagonal bands which, in the case that isospin symmetry is conserved in the πN system, should have a common overlap with the ellipses resulting from the combined fits to the elastic-scattering data.

Using a different approach (and a different algorithm for the electromagnetic corrections), the authors have come to similar conclusions. Their results have been based on a small subset of the existing πN data base.

C. Additional remarks

Let us now investigate the extrapolation of the extracted amplitudes $f_{\pi^+p}(\epsilon)$, $f_{\pi^-p}(\epsilon)$, and $f_{\text{SCX}}(\epsilon)$ to threshold. The

results will be compared either with experimental information directly obtained there or with extrapolations based on *single-channel* analyses.

(a) π^+p : $b_0 + b_1 = -0.0769 \pm 0.0026 \text{ m}_\pi^{-1}$. The extrapolated value is identical to the one obtained in Ref. [41] ($-0.0771 \pm 0.0033 \text{ m}_\pi^{-1}$) with a different method (an extended threshold expansion of the K matrix) and on the basis of the recent measurements exclusively; this fact serves as a

good indication that the model dependence of the results, obtained herein, is small.

(b) π^-p : $b_0 - b_1 = 0.0826 \pm 0.0020 m_\pi^{-1}$. The extrapolated value is about 7% below the experimentally obtained one in Ref. [48] ($0.0885 \pm 0.0009 m_\pi^{-1}$); if not due to trivial effects, this difference might also manifest isospin breaking in the πN system.

(c) SCX: $b_1 = -0.0827 \pm 0.0015 m_\pi^{-1}$. The experimental value, obtained in Ref. [48], is $-0.096 \pm 0.007 m_\pi^{-1}$. Siegel and Gibbs [49] have also extracted a b_1 value from low-energy SCX data; the authors have made use of a coupled-channel approach with nonlocal potentials. Their value ($-0.097 \pm 0.003 m_\pi^{-1}$) is incompatible with the result of the present work. However, a particular form for the (real part of the) πN scattering amplitude is assumed in Ref. [49] for the extrapolation to threshold (from the energy corresponding to the experimental data); the p -wave component is considered to be proportional to $k^2 \cos(\theta)$ (θ denotes the c.m. scattering angle). This is equivalent to assuming that the p -wave isovector coefficient c_1 of the πN scattering amplitude is a constant in the low-energy region (e.g., below 50 MeV). As deduced from Fig. 4 of Ref. [3], this assumption may not be safe.

Provided that the isospin breaking, reported herein, is not created by trivial effects (i.e., gross experimental errors or largely erroneous electromagnetic corrections), then values of the low-energy hadronic constants might not be meaningful, unless the type of the corresponding input data base is adequately specified. A detailed accounting of all the model parameters is in preparation [50]; in the present work reported are only values of $g_{\pi NN}$, due to the broad interest this coupling constant receives also from other research domains in Physics. One may argue that what is determined in the present approach from π^+p data is the coupling constant g_{π^+pn} , whereas the π^-p data lead to the determination of g_{π^-pn} ; both g_{π^0pp} and g_{π^0nn} are involved in the SCX reaction. The combined fits to elastic-scattering data yield $g_{\pi^\pm pn}$, i.e., an ‘‘average’’ value of $g_{\pi NN}$ over the two elastic-scattering channels. Strictly speaking, one should refer to one coupling constant $g_{\pi NN}$, only if all these values are compatible. It was indeed found that the $g_{\pi NN}$ values for the four classes of fits of Sec. IV C agree (within the uncertainties). The ‘‘average’’ value $g_{\pi^\pm pn}$ is equal to 13.18 ± 0.12 .⁶ The fits to the SCX data yield a value of 12.95 ± 0.31 .

A compilation of pre-meson-factory $g_{\pi NN}$ values may be found in Refs. [51]. The value, extracted in Ref. [52], was found to reproduce the πN experimental data in the KH80 analysis [4]. Recent literature values for the πNN coupling constant are listed in Table I (along with the values extracted in the present work) in the more familiar form:

$$f_{\pi NN}^2 = \left(\frac{m_\pi}{2m}\right)^2 \frac{g_{\pi NN}^2}{4\pi}. \quad (8)$$

⁶The $g_{\pi^\pm pn}$ value, obtained after the measurements of Refs. [16] and [24] were entirely removed from the data base, is equal to 13.19 ± 0.09 .

TABLE I. The values of the πNN coupling constant obtained in the present analysis (from the combined $\pi^\pm p$ fits and from the SCX fits) in comparison with values obtained in other recent works. Notice that these values originate from analyses of πN , as well as NN and $\bar{N}N$ data.

Reference	Data base	$f_{\pi NN}^2$	Vertex type
This work	$\pi^\pm p$	$(76.5 \pm 1.4)10^{-3}$	$\pi^\pm pn$
This work	SCX	$(73.9 \pm 3.5)10^{-3}$	Mixed
[4]	πN	$(79 \pm 1)10^{-3}$	πNN
[53]	πN	$(77.1 \pm 1.4)10^{-3}$	πNN
[54]	πN	$(76 \pm 1)10^{-3}$	πNN
[55]	np	$(74.8 \pm 0.3)10^{-3}$	$\pi^\pm pn$
[55]	pp	$(74.5 \pm 0.6)10^{-3}$	$\pi^0 pp$
[55]	$\bar{p}p$	$(73.2 \pm 1.1)10^{-3}$	$\pi^\pm pn$
[56]	np	$(75.7 \pm 0.8 \pm 1.3)10^{-3}$	$\pi^\pm pn$
[56]	pp	$(77.1 \pm 0.9 \pm 0.4)10^{-3}$	$\pi^0 pp$
[57]	$\bar{p}p$	$(71 \pm 2)10^{-3}$	$\pi^\pm pn$

One should remark that these values originate from analyses of πN (Refs. [4,53,54], and the present work), as well as NN and $\bar{N}N$ data (the current values from the Nijmegen group [55], and the values of Refs. [56] and [57]). The result of Ref. [58] has not been included in Table I because it was recently revised [59] and the new value is still considered to be preliminary [60]; this value is in agreement with Ref. [4]. With the exception of the values of Refs. [4] and [57], general agreement is observed in the entries of Table I.

VI. SUMMARY AND CONCLUSIONS

The aim of the present analysis was to test the principle of isospin symmetry of the strong interaction in the πN system. This was achieved by analyzing the low-energy (20–100 MeV) πN data within the context of a relativistic isospin-symmetric πN interaction model. Separate fits to the measurements in the three low-energy experimentally accessible channels were carried out and the corresponding scattering amplitudes were extracted. The present work leads to the following conclusions:

(a) The low-energy πN data base is internally consistent in case where one rejects the true outliers mostly contained in the π^+p channel.

(b) Isospin symmetry in the πN system is clearly violated at low energies; the three low-energy experimentally accessible reactions cannot be simultaneously described within the framework of the parametric model.

(c) The effect pertains to the s -wave part of the interaction.

On the basis of these findings, the following comments are pertinent:

(a) The determination of the low-energy hadronic constants (including the $\pi N \Sigma$ term) from πN data must be carefully reconsidered.

(b) Dispersion-relation analyses in the πN sector have to be appropriately revised taking into account the results of the present work.

(c) Assuming that the calculations within the framework of the chiral-perturbation theory will be extended to the en-

ergies corresponding to the scattering data, then a new value for the u - and d -quark mass difference may be obtained from the πN measurements.

The validity of the present work relies on two basic assumptions. (a) The bulk of the low-energy πN experimental data is correct. (b) The electromagnetic corrections of Ref. [37] are not largely erroneous.

ACKNOWLEDGMENTS

I would like to thank H. J. Leisi for his constant interest in this work. I acknowledge helpful discussions with A. Badertscher, D. V. Bugg, P. F. A. Goudsmit, G. Höhler, M. Janousch, R. Machleidt, G. C. Oades, G. Rasche, M. Sainio, D. Wyler, and Z. G. Zhao. I am indebted to J. T. Brack and E. Friedman for sharing their experimental data with me prior to publication. My attention to the usefulness of the robust statistics in this problem was eventually drawn due to the efforts of N. Fettes and D. Sigg. Last but not least, I would like to thank W. A. Stahel for an abundance of electronic mail on issues of Statistics.

APPENDIX

1. Isospin symmetry in the πN system

The notion of isospin symmetry originated from the observation that, as far as the nuclear forces are concerned, the proton and the neutron behave as degenerate states of one entity, i.e., of the nucleon. A quantum number, called isotopic spin or isospin, $I (= 1/2)$ was assigned to the nucleon; its third component I_z distinguishes between the proton ($I_z = 1/2$) and the neutron ($I_z = -1/2$) state. An isospin of 1 was assigned to the pion, since it comes in three charge states: π^+ ($I_z = 1$), π^- ($I_z = -1$), and π^0 ($I_z = 0$).

Conservation of isospin in the πN system means that the strong-interaction component in the πN scattering amplitude depends only on the total-isospin value I (of the πN system). The direct implication is that, in such a case, all possible low-energy πN reactions can be described by two amplitudes (per spin-parity channel); these amplitudes correspond to the two possibilities of combining an isospin-1 and an isospin-1/2 field, thus, leading to total isospin $I = 3/2$ or $I = 1/2$.

Let us consider the $I = 3/2$ states first. Evidently, the state with $I_z = 3/2$ corresponds to the $\pi^+ p$ system. Therefore,

$$\left| \frac{3}{2} \frac{3}{2} \right\rangle = |\pi^+ p\rangle = |1 1\rangle \left| \frac{1}{2} \frac{1}{2} \right\rangle.$$

Applying the isospin-lowering operator on both sides, one obtains

$$\left| \frac{3}{2} \frac{1}{2} \right\rangle = \sqrt{\frac{2}{3}} |1 0\rangle \left| \frac{1}{2} \frac{1}{2} \right\rangle + \frac{1}{\sqrt{3}} |1 1\rangle \left| \frac{1}{2} -\frac{1}{2} \right\rangle.$$

Similarly,

$$\left| \frac{3}{2} -\frac{1}{2} \right\rangle = \frac{1}{\sqrt{3}} |1 -1\rangle \left| \frac{1}{2} \frac{1}{2} \right\rangle + \sqrt{\frac{2}{3}} |1 0\rangle \left| \frac{1}{2} -\frac{1}{2} \right\rangle$$

and

$$\left| \frac{3}{2} -\frac{3}{2} \right\rangle = |\pi^- n\rangle = |1 -1\rangle \left| \frac{1}{2} -\frac{1}{2} \right\rangle.$$

Two states with total isospin $I = 1/2$ exist; they correspond to $I_z = 1/2$ and $I_z = -1/2$. One may write

$$\left| \frac{1}{2} \frac{1}{2} \right\rangle = \alpha |1 0\rangle \left| \frac{1}{2} \frac{1}{2} \right\rangle + \beta |1 1\rangle \left| \frac{1}{2} -\frac{1}{2} \right\rangle$$

and

$$\left| \frac{1}{2} -\frac{1}{2} \right\rangle = \gamma |1 -1\rangle \left| \frac{1}{2} \frac{1}{2} \right\rangle + \delta |1 0\rangle \left| \frac{1}{2} -\frac{1}{2} \right\rangle.$$

The coefficients α , β , γ , and δ can be determined with the help of the orthogonality and normalization conditions. Omitting an uninteresting phase factor, one may write

$$\left| \frac{1}{2} \frac{1}{2} \right\rangle = \pm \frac{1}{\sqrt{3}} |1 0\rangle \left| \frac{1}{2} \frac{1}{2} \right\rangle \mp \sqrt{\frac{2}{3}} |1 1\rangle \left| \frac{1}{2} -\frac{1}{2} \right\rangle$$

and

$$\left| \frac{1}{2} -\frac{1}{2} \right\rangle = \pm \sqrt{\frac{2}{3}} |1 -1\rangle \left| \frac{1}{2} \frac{1}{2} \right\rangle \mp \frac{1}{\sqrt{3}} |1 0\rangle \left| \frac{1}{2} -\frac{1}{2} \right\rangle.$$

Eventually, after selecting the upper signs (the results do not depend on the sign convention),

$$|1 -1\rangle \left| \frac{1}{2} \frac{1}{2} \right\rangle = |\pi^- p\rangle = \frac{1}{\sqrt{3}} \left| \frac{3}{2} -\frac{1}{2} \right\rangle + \sqrt{\frac{2}{3}} \left| \frac{1}{2} -\frac{1}{2} \right\rangle$$

and

$$|1 0\rangle \left| \frac{1}{2} -\frac{1}{2} \right\rangle = |\pi^0 n\rangle = \sqrt{\frac{2}{3}} \left| \frac{3}{2} -\frac{1}{2} \right\rangle - \frac{1}{\sqrt{3}} \left| \frac{1}{2} -\frac{1}{2} \right\rangle.$$

As already mentioned, the assumption that the strong interaction is isospin symmetric means that the strong amplitude finally depends only on the total isospin of the πN system. This implies that the isospin component of the πN wave function obeys the forms

$$|\pi^+ p\rangle = \left| \frac{3}{2} \right\rangle, \quad |\pi^- p\rangle = \frac{1}{\sqrt{3}} \left| \frac{3}{2} \right\rangle + \sqrt{\frac{2}{3}} \left| \frac{1}{2} \right\rangle,$$

and

$$|\pi^0 n\rangle = \sqrt{\frac{2}{3}} \left| \frac{3}{2} \right\rangle - \frac{1}{\sqrt{3}} \left| \frac{1}{2} \right\rangle.$$

Let us now construct the hadronic amplitudes $f_{\pi^+ p}(\epsilon)$, $f_{\pi^- p}(\epsilon)$, and $f_{\text{SCX}}(\epsilon)$ corresponding to the two elastic $\pi^+ p$, $\pi^- p$, and to the SCX reaction, respectively; ϵ denotes the center-of-mass (c.m.) kinetic energy of the incident pion.

$$f_{\pi^+ p}(\epsilon) = \langle \pi^+ p | H | \pi^+ p \rangle = f_3(\epsilon),$$

where H is the Hamiltonian operator and $f_3(\epsilon)$ denotes the amplitude in the $I = 3/2$ channel. Similarly,

$$f_{\pi^-p}(\epsilon) = \langle \pi^- p | H | \pi^- p \rangle = \frac{f_3(\epsilon) + 2f_1(\epsilon)}{3}$$

and

$$f_{\text{scx}}(\epsilon) = \langle \pi^0 n | H | \pi^- p \rangle = \sqrt{2} \frac{f_3(\epsilon) - f_1(\epsilon)}{3},$$

where $f_1(\epsilon)$ stands for the amplitude in the $I=1/2$ channel. The values of the amplitudes $f_3(\epsilon)$ and $f_1(\epsilon)$ at threshold ($\epsilon=0$ MeV) are the s -wave scattering lengths a_3 and a_1 , respectively.

Combining the last three equations, one obtains the so-called *triangle identity*:

$$f_{\text{scx}}(\epsilon) = \frac{1}{\sqrt{2}} [f_{\pi^+p}(\epsilon) - f_{\pi^-p}(\epsilon)].$$

2. Special features of the πN amplitude in the low-energy region

At low energies, only the s - and p -wave contributions to (the strong-interaction part of) the πN scattering amplitude

are important; therefore, the most general form of the operator (from which the scattering amplitude for a particular reaction may be constructed), respecting parity conservation, rotational, and isospin symmetry, is given by the following formula, introduced in Ref. [61]:

$$f_{\pi N}(\epsilon) = [b_0(\epsilon) + b_1(\epsilon) \boldsymbol{\tau} \cdot \mathbf{t}] + [c_0(\epsilon) + c_1(\epsilon) \boldsymbol{\tau} \cdot \mathbf{t}] \mathbf{k}_f \cdot \mathbf{k}_i + [d_0(\epsilon) + d_1(\epsilon) \boldsymbol{\tau} \cdot \mathbf{t}] i \boldsymbol{\sigma} \cdot (\mathbf{k}_f \times \mathbf{k}_i), \quad (\text{A1})$$

where \mathbf{k}_i and \mathbf{k}_f stand for the c.m. momenta of the incident and outgoing pion, respectively, and \mathbf{t} denotes the pion isospin operator; $\boldsymbol{\tau}/2$ and $\boldsymbol{\sigma}/2$ are the nucleon isospin and spin operators. The coefficients $b_0(\epsilon), \dots, d_1(\epsilon)$ are complex; their imaginary parts are small in the energy region considered in the present work, and vanish at the πN threshold. The s -wave part of the interaction is contained in the coefficients $b_0(\epsilon)$ and $b_1(\epsilon)$; the remaining coefficients pertain to the p -wave component. The quantities $b_0(\epsilon)$ and $b_1(\epsilon)$ at threshold are, respectively, the isoscalar and isovector s -wave scattering lengths and are simply denoted by b_0 and b_1 .

-
- [1] S. Weinberg, in *Chiral Dynamics: Theory and Experiment, Proceedings of the Workshop held at MIT*, Cambridge, MA, 1994, edited by A. M. Bernstein and B. R. Holstein (Springer, Berlin, 1995), p. 3; H. Leutwyler, *ibid.*, p. 14.
- [2] V. Bernard, N. Kaiser, and Ulf-G. Meissner, *Phys. Rev. C* **52**, 2185 (1995).
- [3] P. F. A. Goudsmit, H. J. Leisi, E. Matsinos, B. L. Birbrair, and A. B. Gridnev, *Nucl. Phys.* **A575**, 673 (1994).
- [4] R. Koch and E. Pietarinen, *Nucl. Phys.* **A336**, 331 (1980).
- [5] R. M. Barnett *et al.*, *Phys. Rev. D* **54**, 1 (1996).
- [6] N. A. Törnqvist and M. Roos, *Phys. Rev. Lett.* **76**, 1575 (1996).
- [7] P. J. Bussey, J. R. Carter, D. R. Dance, D. V. Bugg, A. A. Carter, and A. M. Smith, *Nucl. Phys.* **B58**, 363 (1973).
- [8] J. S. Frank *et al.*, *Phys. Rev. D* **28**, 1569 (1983).
- [9] J. T. Brack *et al.*, *Phys. Rev. C* **34**, 1771 (1986).
- [10] J. T. Brack, J. J. Kraushaar, D. J. Rilett, R. A. Ristinen, D. F. Ottewell, G. R. Smith, R. G. Jeppesen, and N. R. Stevenson, *Phys. Rev. C* **38**, 2427 (1988).
- [11] U. Wiedner *et al.*, *Phys. Rev. D* **40**, 3568 (1989).
- [12] J. T. Brack *et al.*, *Phys. Rev. C* **41**, 2202 (1990).
- [13] J. T. Brack *et al.*, *Phys. Rev. C* **51**, 929 (1995).
- [14] Ch. Joram *et al.*, *Phys. Rev. C* **51**, 2144 (1995); Ch. Joram *et al.*, *ibid.* **51**, 2159 (1995).
- [15] M. Janousch, A. Badertscher, P. F. A. Goudsmit, H. J. Leisi, E. Matsinos, P. Weber, and Z. G. Zhao, "Destructive interference of s and p waves in $180^\circ \pi^- p$ elastic scattering," ETHZ-IPP Report No. 97-03 (1997).
- [16] P. Y. Bertin *et al.*, *Nucl. Phys.* **B106**, 341 (1976).
- [17] E. G. Auld *et al.*, *Can. J. Phys.* **57**, 73 (1979).
- [18] B. G. Ritchie, R. S. Moore, B. M. Freedom, G. Das, R. C. Minehart, K. Gotow, W. J. Burger, and H. J. Ziock, *Phys. Lett.* **125B**, 128 (1983).
- [19] U. Wiedner (private communication).
- [20] E. Friedman, A. Goldring, G. J. Wagner, A. Altman, R. R. Johnson, O. Meirav, and B. K. Jennings, *Nucl. Phys.* **A514**, 601 (1990).
- [21] E. Friedman (private communication).
- [22] E. Friedman (private communication); M. M. Pavan, *πN Newsletter* **11**, 117 (1995).
- [23] B. J. Kriss *et al.*, *πN Newsletter* **12**, 20 (1997).
- [24] A. A. Carter, J. R. Williams, D. V. Bugg, P. J. Bussey, and D. R. Dance, *Nucl. Phys.* **B26**, 445 (1971).
- [25] E. Pedroni *et al.*, *Nucl. Phys.* **A300**, 321 (1978).
- [26] R. Wieser *et al.*, *Phys. Rev. C* **54**, 1930 (1996).
- [27] J. C. Alder *et al.*, *Phys. Rev. D* **27**, 1040 (1983).
- [28] M. E. Sevier *et al.*, *Phys. Rev. C* **40**, 2780 (1989).
- [29] D. H. Fitzgerald *et al.*, *Phys. Rev. C* **34**, 619 (1986).
- [30] J. Duclos *et al.*, *Phys. Lett.* **43B**, 245 (1973).
- [31] M. Salomon, D. F. Measday, J.-M. Poutissou, and B. C. Robertson, *Nucl. Phys.* **A414**, 493 (1984).
- [32] A. Bagheri, K. A. Aniol, F. Entezami, M. D. Hasinoff, D. F. Measday, J.-M. Poutissou, M. Salomon, and B. C. Robertson, *Phys. Rev. C* **38**, 885 (1988).
- [33] D. V. Bugg, P. J. Bussey, D. R. Dance, A. R. Smith, A. A. Carter, and J. R. Williams, *Nucl. Phys.* **B26**, 588 (1971).
- [34] B. Bassalleck (private communication); B. Bassalleck, *πN Newsletter* **8**, 150 (1993).
- [35] D. Isenhower (private communication).
- [36] D. Počanić (private communication).
- [37] B. Tromborg, S. Waldenström, and I. Överbø, *Phys. Rev. D* **15**, 725 (1977); *Helv. Phys. Acta* **51**, 584 (1978).
- [38] D. V. Bugg, *πN Newsletter* **2**, 15 (1990); J. S. Frank, *ibid.* **2**, 21 (1990); D. V. Bugg, *ibid.* **3**, 1 (1991); G. Smith, *ibid.* **5**, 108 (1992); D. V. Bugg, *ibid.* **6**, 139 (1992); J. T. Brack, *ibid.* **6**, 144 (1992).

- [39] F. R. Hampel, E. M. Ronchetti, P. J. Rousseeuw, and W. A. Stahel, *Robust Statistics* (Wiley, New York, 1986).
- [40] F. James and M. Roos, "MINUIT, Function Minimization and Error Analysis," CERN Report No. D506 (1994).
- [41] N. Fettes and E. Matsinos, *Phys. Rev. C* **55**, 464 (1997).
- [42] R. E. Cutkosky, *Phys. Lett.* **88B**, 339 (1979).
- [43] W. B. Kaufmann and W. R. Gibbs, *Ann. Phys. (N.Y.)* **214**, 84 (1992).
- [44] B. L. Birbrair and A. B. Gridnev, *Phys. Lett.* **335B**, 6 (1994).
- [45] E. Matsinos, "The low-energy πN elastic-scattering data," ETHZ-IPP Report No. 97-04 (1997).
- [46] A. Badertscher *et al.*, "Is Isospin Symmetry violated in the Pion-Nucleon Sector at Threshold?" ETHZ-IPP Report No. 94-10 (1994); H. J. Leisi *et al.*, in *Chiral Dynamics: Theory and Experiment* (Ref. [1]), p. 241.
- [47] W. R. Gibbs, Li Ai, and W. B. Kaufmann, *Phys. Rev. Lett.* **74**, 3740 (1995).
- [48] D. Sigg *et al.*, *Nucl. Phys.* **A609**, 269 (1996); D. Sigg, A. Badertscher, P. F. A. Goudsmit, H. J. Leisi, and G. C. Oades, *ibid.* **A609**, 310 (1996); D. Sigg *et al.*, *Phys. Rev. Lett.* **75**, 3245 (1995).
- [49] P. B. Siegel and W. R. Gibbs, *Phys. Rev. C* **33**, 1407 (1986).
- [50] E. Matsinos (unpublished).
- [51] M. M. Nagels *et al.*, *Nucl. Phys.* **B147**, 189 (1979); O. Dumbrajs, R. Koch, H. Pilkuhn, G. C. Oades, H. Behrens, J. J. de Swart, and P. Kroll, *ibid.* **B216**, 277 (1983).
- [52] D. V. Bugg, A. A. Carter, and J. R. Carter, *Phys. Lett.* **44B**, 278 (1973).
- [53] F. G. Markopoulou-Kalamara and D. V. Bugg, *Phys. Lett. B* **318**, 565 (1993).
- [54] R. A. Arndt, R. L. Workman, and M. M. Pavan, *Phys. Rev. C* **49**, 2729 (1994).
- [55] R. G. E. Timmermans, *Few-Body Syst., Suppl.* **9**, 169 (1995); *πN Newsletter* **11**, 7 (1995).
- [56] D. V. Bugg and R. Machleidt, *Phys. Rev. C* **52**, 1203 (1995).
- [57] F. Bradamante, A. Bressan, M. Lamanna, and A. Martin, *Phys. Lett. B* **343**, 431 (1995).
- [58] T. E. O. Ericson *et al.*, *Phys. Rev. Lett.* **75**, 1046 (1995).
- [59] T. Ericson and B. Loiseau, *Phys. Lett. B* **393**, 167 (1997).
- [60] T. E. O. Ericson, B. Loiseau, J. Blomgren, and N. Olsson, *πN Newsletter* **12**, 16 (1997).
- [61] M. Ericson and T. E. O. Ericson, *Ann. Phys. (N.Y.)* **36**, 323 (1966).